jet INTL JOURNAL OF ELECTRONICS AND TELECOMMUNICATIONS, 2018, VOL. 64, NO. 4, PP. 497–503
Manuscript received February 21, 2018; revised October, 2018. DOI: 10.24425/123551

Energy Efficiency Optimization by Spectral Efficiency Maximization in 5G Networks

Bujar Krasniqi, Blerim Rexha* and Betim Maloku

***Abstract*—Energy and spectral efficiency are the main challenges in 5th generation of mobile cellular networks. In this paper, we propose an optimization algorithm to optimize the energy efficiency by maximizing the spectral efficiency. Our simulation results show a significant increase in terms of spectral efficiency as well as energy efficiency whenever the mobile user is connected to a low power indoor base station. By applying the proposed algorithm, we show the network performance improvements up to 9 bit/s/Hz in spectral efficiency and 20 Gbit/Joule increase in energy efficiency for the mobile user served by the indoor base station rather than by the outdoor base station.**

***Keywords*—Energy efficiency, 5G, radio resources, power allocation, optimization convexity**

I. Introduction

THE 4G had initially promised to offer high data rate as well as low data latency. However, the real needs and current technical services are still far away to meet the users' demands and satisfaction. The reports of mobile operators around the world, indicate that 4G users consume up to three times more data compared to non-4G users. One of the key factors in increasing the data consumption is video streaming. In the next six years, more than 1 million new mobile subscibers will be added per day, resulting in 2.6 billion subscribers by the end of 2022 [1]. It is predicted that the total daily mobile traffic in the Western European countries in years from 2010 to 2020 will increase from 186 TBs (terabytes) to 12540 TBs, thus resulting in 67 times higher daily traffic [2]. At the end of 2016 the global mobile data traffic reached 7.2 exabytes per month [3].

The current wireless systems are far from providing the substantial traffic increase due to the requirements from applications as fast remote access to the cloud, high speed data for video streaming etc. Furthermore, the energy efficiency (EE) is low as the most power consumption of base stations (BSs) is used to meet the threshold of pathloss. The fifth generation (5G) of mobile networks, which is expected to meet high end requirements [4] and be deployed by 2020, is supposed to provide approximately 1000 times higher the data rates, 90% savings up of the energy expense per service, ten times higher battery life time of connected devices, more than 1000 Gbit/s/km2 spectral efficiency (SE) in dense urban areas, and 5 times less end-to-end latency compared to 4G [5].

A fundamental study on the trade-off between EE and SE for the scenario with and without hardware properties was done by authors in [6]. For an OFDMA system [7] the EE was shown to be quasi convex in SE. The trade-off between EE and SE is applied in different scenarios [8], [9]. A new design framework which tries to balance the SE and EE in a 5G wireless system is done by authors in [10]. According to [5], an ultra-densification of access nodes is indispensable to meet such requirements. With an enormous increase of access nodes, the total energy consumption will increase too, where a large amount of total energy expense goes for the energy radiated by antennas. Thus, to make the 5G network more efficient in terms of energy consumption, the power allocated to the BSs should be optimized [11]. There have been some works in this direction, for example [12], [13], [14], [15], [16], [17], [18], applying different techniques, but none of them formulated an optimization algorithm which increases the efficiency of the network by maximizing the spectral efficiency under optimal power allocation to the BS.

To address this challenging problem, we present a unique solution that optimizes the EE by maximizing the SE under optimal power allocation. This solution considers a specific scenario as part of a 5G network. Furthermore, we have analyzed the trade-off between EE and SE for indoor and outdoor environments.

The paper is organized as follows. In Section II, the geometry of the system model is presented together with the pathloss attenuation models for indoor and outdoor user's environment. In Section III, we have formulated the SE optimization problem and solved it by using Water-Filling-Like method for power allocation. In Section IV, we present the simulation results and finally the Section V concludes the work.

II. System Model

In our system model, we consider seven micro outdoor base stations (OBSs), each equipped with three sector antennas, thus yielding three cells per site. In each cell, indoor base stations (IBSs) are randomly distributed. The system model is illustrated in Fig. 1.

The mobile user is served always by the micro OBS, expect the case when the users' pathloss attenuation is

B. Krasniqi and B. Rexha* are with University of Prishtina, Faculty of Electrical and Computer Engineering, Prishtina, 10000 Kosovo (e-mail: blerim.rexha@uni-pr.edu).
B. Maloku is with Vienna University of Technology.

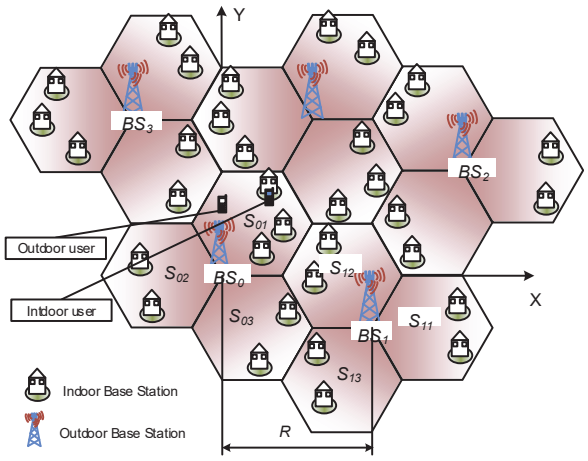

Fig. 1. 5G system model with OBSs and IBSs.

smaller than indoor pathloss attenuation threshold. In the system model, the mobile users served by IBS are denoted as M^{IBS}, and outdoor users served by OBS are denoted as M^{OBS}. Our cell cluster in the system model is organized in hexagonal grid with a center BS, denoted as BS_0 and its three sectors denoted as S_{01}, S_{02} and S_{03}, where index 0 denotes BS_0 and indexes 1, 2 and 3 denote first, second and third sector, respectively. Outdoor users which are located in the coverage area of sector S_{01} of OBS BS_0 receive power from sector S_{01}, and interference from two other sectors (S_{02} and S_{03}) of their serving OBS, and from all sectors (S_{k1}, S_{k2} and S_{k3}) of other OBSs, BS_k, where $k = 1, 2, 3, 4, 5, 6$. Considering the fact that the transmit power of an IBS is low compared to the transmit power of OBS, the interference from IBSs is neglected. The spectral efficiency $\eta^{OBS}_{SE(m)}$ of an outdoor user m located in sector S_{01} is defined as in [19],

$$\eta^{OBS}_{SE(m)} = \frac{R^{OBS}_m}{B^{OBS}_0}, \tag{1}$$

where R^{OBS}_m denotes the transmission rate, and B^{OBS}_0 is the allocated bandwidth for the randomly chosen outdoor user m.

The data rate achieved by an outdoor user m located in sector S_{01} is defined as in [20],[21], [22]

$$R^{OBS}_m = B^{OBS}_m \log_2 \left(1 + \frac{G^{OBS}_{0m} p^{OBS}_0}{N_0 B^{OBS}_m + \sum_{k=1}^{6} G^{OBS}_{km} p^{OBS}_k} \right), \tag{2}$$

where p^{OBS}_m represents the transmit power assigned to the outdoor user m, N_0 is the noise spectral density, and p^{OBS}_k is the interference power. The direct channel pathloss attenuation coefficient of the desired channel is denoted with G^{OBS}_{0m} while the interference channels pathloss attenuation is represented by G^{OBS}_{km}. The Equation for the pathloss models of desired and interfering channels is defined in (5). Similarly to the outdoor users, the indoor users which belong to sector S_{01} of OBS BS_0 receive power from IBS located in this sector, and interference from all sectors (S_{k1}, S_{k2} and S_{k3}) of OBSs, BS_k, where $k = 0, 1, 2, 3, 4, 5, 6$. Assuming the effect of wall penetration loss and that the transmit power of IBS which is low compared to the transmit power of OBSs, we neglect the interference from other IBSs. The spectral efficiency denoted as η^{IBS}_m of an randomly choosen indoor user m located in sector S_{01} is defined as

$$\eta^{IBS}_{SE(m)} = \frac{R^{IBS}_m}{B^{IBS}_0}, \tag{3}$$

where R^{IBS}_m denotes the transmission rate, and B^{IBS}_0 is the bandwith allocated to an indoor user m. The transmission rate achieved by an indoor user m located in sector S_{01} is defined as [20],[21], [22]

$$R^{IBS}_m = B^{IBS}_m \log_2 \left(1 + \frac{G^{IBS}_{0m} p^{IBS}_0}{N_0 B^{IBS}_m + \sum_{k=1}^{6} G^{IBS}_{km} p^{IBS}_k} \right), \tag{4}$$

where p^{IBS}_m denotes the transmit power assigned to the indoor user m, N_0 represents the noise spectral density, and p^{IBS}_k is the interference power from neighbor OBSs, i.e. $p^{IBS}_k = p^{OBS}_k$, to avoid notation definitions. The coefficients G^{IBS}_{0m} and G^{IBS}_{km} denote the pathloss model of the desired channel and interfering channels, respectively. The indoor pathloss model for desired channel is defined by Equation (6), while the indoor pathloss model for interference channels is expressed by Equation (7).

A. Pathloss Attenuation Models

As it is known, due to the movement of the Receiver (Rx) and also of the surrounding objects, the wireless channel is not time invariant. From the measurements realized for vehicular and non-vehicular users in lower frequencies such as 800 MHz, 1800 MHz and 2600 MHz [23], [24], [25], [26], we found that penetration loss is different for inside and outside users. So different pathloss models are necessary to be considered for indoor and outdoor users. To consider the effects of a time variant wireless channel, we use an improved version of pathloss model given in [27]. Two factors that characterize the propagation environment are the antenna gain and small-scale fading. The pathloss model (PLM) for a desired channel of the outdoor users is expressed as

$$G^{OBS}_{km} = -[79.2 + 26 \log_{10} d + X_\sigma - A^{OBS} + F] \tag{5}$$

where d represents the distance between outdoor user and base station in m, X_σ is the log-normal shadowing in dB, A^{OBS} is the sum of outdoor user antenna gain and OBS antenna gain in dBi and F denotes the small-scale fading in dB. The constants 79.2 and 26 are specific for the center frequency of 28 GHz. The pathloss model for the interfering channel of outdoor users is similar as in (5), except that the small-scale

fading F is not taken into account. The indoor PLM for the desired channel of indoor users is expressed as in [28]

$$G_{0m}^{IBS} = -[20\log_{10} f + N\log_{10} d + P_f(n) - 28] \quad (6)$$

where f is the center frequency in MHz, N is the distance power loss coefficient expressed as natural number, d denotes the distance between indoor user and IBS in m, $P_f(n)$ is the floor penetration loss factor in dB and n is the number of floors between indoor user and indoor access point expressed as natural number.

The indoor PLM for the interfering channel of indoor users is defined similarly as in Equation (5), except that small-scale fading F is not taken into account and a penetration loss factor L_{pen} which is added, as given in Equation (7).

$$G_{km}^{IBS} = -[79.2{+}26\log_{10} d{+}X_\sigma{-}A^{IBS}{+}L_{pen}] \quad (7)$$

where A^{IBS} denotes the sum of indoor user antenna gain and OBS antenna gain in dBi [21] and L_{pen} is the penetration wall loss in dB.

III. Energy Efficiency Optimization Algorithms

During a soft handover and provided its properties in mobile communication system, a mobile user is able to be simultaneously connected to more than one BS. However, the mobile network will decide for a mobile user from which BS to be served. In our model, the decision for users service is performed based on comparison of received pathloss attenuation form OBS and IBS. Algorithm 1 decides whether a mobile user will be served by OBS or IBS (see below for the details of this algorithm).

Algorithm 1 Algorithm for User Classification

Measure: $PLA, IPLA$

if $PLA < IPLA$ **then**
  Indoor User → IBS
else
  Outdoor User → OBS
end if
Calculate:
$p_0^{IBS}, p_k^{IBS}, p_0^{OBS}, p_k^{OBS}$
using Equation (9) for power allocation.

In an OBS and IBS scenario, the mobile network measures the PLA and IPLA at the mobile user. Depending on channel conditions of mobile user, the Algorithm 1 classifies a user as an indoor user as a result that the user is connected to IBS, otherwise the user will be connected to OBS. After user selection, the Water-filling like power allocation algorithm is used to optimally allocate the power to the IBS and OBS in order to maximize the SE. The optimization problem which optimizes the SE depends on transmit power and bandwidth assignment and is given as in the following

$$\underset{p^{OBS},p^{IBS},B^{OBS},B^{IBS}}{\text{maximize}} \quad \eta_{SE}^{OBS} + \eta_{SE}^{IBS} \quad (8a)$$

subject to

$$\alpha_{IBS}p_0^{OBS} + \alpha_{OBS}p_0^{IBS} \le P^{max} \quad (8b)$$

$$B^{OBS} + B^{IBS} = B^{max}, \quad (8c)$$

$$p^{OBS} \ge 0, \quad (8d)$$

$$p^{IBS} \ge 0, \quad (8e)$$

$$B^{OBS} \ge 0, \quad (8f)$$

$$B^{IBS} \ge 0. \quad (8g)$$

The coefficients α_{IBS} and α_{OBS} in the constraint (8b), are used to express the portion of transmit power assigned from IBS and OBS, respectively. As the SE maximization is a constrained optimization problem, shown in Equation (8), in standard power control as a particular case [20], the SE maximization problem is not convex. Assuming that the outdoor user is served with equal power and interference from OBSs and the indoor user does not experience interference due to low power of IBSs, the SE maximization problem is solvable by Water-filling Like method as it is transformed to a convex problem. The optimization problem formulated in Equation (8) can be extended for the case of multiple users on multiple cells. For simplicity purposes, we focus on a simple scenario with one user which is located within the micro cell on which there are distributed several IBSs. The convexity of the optimization problem formulated in Equation (8) is proved by applying the second derivative of η_{SE}^{OBS} with respect to p_0^{OBS} (results to be concave). Consequently, we obtain that $\hat{\eta}^{OBS}(B_m^{OBS}, p_0^{OBS}) = B_m^{OBS}\eta_{SE}^{OBS}(p_0^{OBS}/B_m^{OBS})$ is concave, since it is the prospect of a concave function [29]. Moreover, as η_{SE}^{IBS} is also concave, due to its logarithmic form [29], the optimization problem in Equation (8) is concave too.

A. Power Allocation using Water-filling-like method

The analytic solution for the optimization problem defined in Equation (8) is not feasible. In order to come to a solution, we further consider that the bandwidth allocation is fixed. By fixing the bandwidth, the algorithm for power allocation can be derived from the Karush-Kuhn-Tucker (KKT) conditions for optimality [29]. For simplicity, we are replacing the variables as in the following

$$\begin{aligned} G_{0m}^{OBS} &= s_m, \\ \sum_{k=1}^{6} G_{km}^{OBS} &= t_m, \\ G_{0m}^{IBS} &= u_m, \\ \sum_{k=0}^{6} G_{km}^{IBS} &= v_m. \end{aligned} \quad (9)$$

We formulate the optimization problem (9) through the Lagrangian as

$$Ł(p^{OBS}, p^{IBS}, \mu, \lambda^{OBS}, \lambda^{IBS}) = \eta_{SE}^{OBS} + \eta_{SE}^{IBS} - \mu(p^{OBS} - P^{max}) - \mu(p^{IBS} - P^{max}) + \lambda^{OBS} p^{OBS} + \lambda^{IBS} p^{IBS}, \tag{10}$$

where the notations μ and λ^{OBS}, λ^{IBS} denote the Lagrange multipliers, μ is the sum-power and λ^{OBS}, λ^{IBS} are the positivity constraints for outdoor and indoor case, respectively.

Applying the KKT conditions we obtain the following inequalities and equalities

$$p^{OBS} \geq 0, \tag{11a}$$
$$p^{IBS} \geq 0, \tag{11b}$$
$$p^{OBS} - P^{max} \leq 0, \tag{11c}$$
$$p^{IBS} - P^{max} \leq 0, \tag{11d}$$
$$\lambda^{OBS} \geq 0, \tag{11e}$$
$$\lambda^{IBS} \geq 0, \tag{11f}$$
$$\lambda^{OBS} p^{OBS} = 0, \tag{11g}$$
$$\lambda^{IBS} p^{IBS} = 0, \tag{11h}$$

$$\frac{\partial L}{\partial p_0^{OBS}} = -\sum_{m=1}^{M^{OBS}} \frac{B_m^{OBS}}{p_0^{OBS} \ln 2} \frac{1}{(N_0 B_m^{OBS} + t_m p_0^{OBS})} \times \frac{s_m N_0 B_m^{OBS}}{[N_0 B_m^{OBS} + (s_m + t_m) p_0^{OBS}]} + \frac{B_m^{OBS}}{(p_0^{OBS})^2} \log_2\left(1 + \frac{s_m}{t_m}\right) + \mu - \lambda^{OBS} = \psi^{OBS}(p_0^{OBS}) - \lambda^{OBS} = 0, \tag{11i}$$

$$\frac{\partial L}{\partial p_0^{IBS}} = -\sum_{m=1}^{M^{IBS}} \frac{B_m^{IBS}}{p_0^{IBS} \ln 2} \frac{1}{(N_0 B_m^{IBS} + \alpha_{OBS} v_m p_0^{IBS})} \times \frac{u_m N_0 B_m^{IBS}}{[N_0 B_m^{IBS} + (u_m + \alpha_{OBS} v_m) p_0^{IBS}]} + \frac{B_m^{IBS}}{(p_0^{IBS})^2} \log_2\left(1 + \frac{u_m}{\alpha_{OBS} v_m}\right) + \mu - \lambda^{IBS} = \psi^{IBS}(p_0^{IBS}) - \lambda^{IBS} = 0. \tag{11j}$$

The equalities (11g) and (11h), derived from the KKT conditions, represent the first derivative of the Lagrangian function expressed by Equation (10) with respect to p_0^{OBS} and p_0^{IBS}, respectively. We obtain the optimal p_0^{OBS} and optimal p_0^{IBS} as function of μ, considering the constraints (11c), (11d), (11e), and (11f), from the roots of functions $\psi^{OBS}(p_0^{OBS})$ and $\psi^{IBS}(p_0^{IBS})$, respectively. The roots of above functions can be calculated using Ferrari-Lagrange method [30]. Considering that $\mu^{OBS} = \sum_{m=1}^{M^{OBS}} [(s_m/(N_0 ln 2)]$ and $\mu^{IBS} = \sum_{m=1}^{M^{IBS}} [(u_m/(N_0 ln 2)]$, the optimal power allocation for the outdoor users and the indoor users is derived as in the following

$$p_0^{OBS} = \begin{cases} p_0^{OBS}(\mu), & \text{if } \frac{1}{\mu} \geq \frac{1}{\mu^{OBS}} \\ 0, & \text{otherwise} \end{cases} \tag{12}$$

$$p_0^{IBS} = \begin{cases} p_0^{IBS}(\mu), & \text{if } \frac{1}{\mu} \geq \frac{1}{\mu^{IBS}} \\ 0, & \text{otherwise.} \end{cases} \tag{13}$$

If $M^{OBS} = 1$ and $M^{IBS} = 1$, the roots shown above can be calculated analytically, thus we obtain the optimal power assigned to the outdoor user as

$$p_0^{OBS} = \left\{ -\frac{k_{31}}{4k_{41}} + Z_1 + \frac{1}{2}\sqrt{-4Z_1^2 - 2\frac{8k_{41}k_{21} - 3k_{31}^2}{8k_{41}^2} - \frac{e_1}{Z_1}}, \right. \tag{14}$$

where parameters e_1, Z_1, Q_1, Δ_{11}, k_{01}, k_{11}, k_{21}, k_{31} and k_{41} are given in the following

$$e_1 = \frac{k_{31}^3 - 4k_{41}k_{31}k_{21} + 8k_{41}^2 k_{11}}{8k_{41}^3},$$

$$Z_1 = \frac{1}{2}\sqrt{-\frac{2}{3}\frac{8k_{41}k_{21} - 3k_{31}^2}{8k_{41}^2} + \delta_1},$$

$$\delta_1 = \frac{1}{3k_{41}}\left(Q_1 + \frac{k_{21}^2 - 3k_{31}k_{11} + 12k_{41}k_{01}}{Q_1}\right)$$

$$Q_1 = \sqrt[3]{\frac{\Delta_{11} + \sqrt{\Delta_{11}^2 - 4(k_{21}^2 - 3k_{31}k_{11} + 12k_{41}k_{01})^3}}{2}}$$

$$\Delta_{11} = 2k_{21}^3 - 9k_{31}k_{21}k_{11} + 27k_{31}^2 k_{01} + 27k_{41}k_{11}^2 - 72k_{41}k_{21}k_{01}$$

$$k_{01} = B_1^{OBS}(N_0 B_1^{OBS})^2 \log_2\left(1 + \frac{s_1}{t_1}\right),$$

$$k_{11} = B_1^{OBS}(N_0 B_1^{OBS}) \left[(s_1 + 2t_1)\log_2\left(1 + \frac{s_1}{t_1}\right) - \frac{s_1}{\ln 2}\right],$$

$$k_{21} = t_1(s_1 + t_1) B_1^{OBS} \log_2\left(1 + \frac{s_1}{t_1}\right) + (N_0 B_1^{OBS})^2 \mu,$$

$$k_{31} = N_0 B_1^{OBS}(s_1 + 2t_1)\mu,$$

$$k_{41} = t_1(s_1 + t_1)\mu.$$

The optimal power assigned to the indoor user is found as in the following

$$p_0^{IBS} = \left\{ -\frac{k_{32}}{4k_{42}} + Z_2 + \frac{1}{2}\sqrt{-4Z_2^2 - 2d_2 - \frac{e_2}{Z_2}}, \quad \text{if } \frac{1}{\mu} \geq \frac{1}{\mu^{IBS}} 0, \right. \tag{15}$$

where parameters e_2, Z_2, Q_2, Δ_{12}, k_{02}, k_{12}, k_{22}, k_{32} and k_{42} are given in the following

$$e_2 = \frac{k_{32}^3 - 4k_{42}k_{32}k_{22} + 8k_{42}^2 k_{12}}{8k_{41}^3},$$

$$Z_2 = \frac{1}{2}\sqrt{-\frac{2}{3}\frac{8k_{42}k_{22} - 3k_{32}^2}{8k_{42}^2} + \delta_2},$$

$$\delta_2 = \frac{1}{3k_{42}}\left(Q_2 + \frac{k_{22}^2 - 3k_{32}k_{12} + 12k_{42}k_{02}}{Q_2}\right)$$

,

$$Q_2 = \sqrt[3]{\frac{\Delta_{12} + \sqrt{\Delta_{12}^2 - 4(k_{22}^2 - 3k_{32}k_{12} + 12k_{42}k_{02})^3}}{2}},$$

$$\Delta_{12} = 2k_{22}^3 - 9k_{32}k_{22}k_{12} + 27k_{32}^2 k_{02} + 27k_{42}k_{12}^2 - 72k_{42}k_{22}k_{02},$$

$$k_{02} = B_1^{IBS}(N_0 B_1^{IBS})^2 \log_2\left(1 + \frac{u_1}{\alpha_{OBS} v_1}\right),$$

$$k_{12} = B_1^{IBS}(N_0 B_1^{IBS})\left[(u_1 + 2\alpha_{OBS} v_1) \times K_1\right],$$

$$K_1 = \log_2\left(1 + \frac{u_1}{\alpha_{OBS} v_1}\right) - \frac{u_1}{\ln 2}$$

$$k_{22} = \alpha_{OBS} v_1 (u_1 + \alpha_{OBS} v_1) B_1^{IBS} \times K_2$$

$$K_2 = \log_2\left(1 + \frac{u_1}{\alpha_{OBS} v_1}\right) + (N_0 B_1^{IBS})^2 \mu,$$

$$k_{32} = N_0 B_1^{IBS} (u_1 + 2\alpha_{OBS} v_1)\mu,$$

$$k_{42} = \alpha_{OBS} v_1 (u_1 + \alpha_{OBS} v_1)\mu.$$

Using the search via simple bisection, the water-filling-level $\frac{1}{\mu}$ reaches the optimum.

IV. Simulations

In this section, we present the simulation results which show the evaluation of the proposed optimization algorithm. The maximum power allocated to OBS and IBS is set to 5 W. We consider 10000 iterations of power allocation and along each iteration of power allocation, 1000 channel realizations are performed. The simulation parameters are presented in Table I.

Applying the simple bisection search in equations (14) and (15), we find the optimal water-filling-level $\frac{1}{\mu}$ and search for the optimal power allocation for both the indoor and outdoor user.

TABLE I
Simulation Parameters

Parameters	Values
Outdoor base station maximum power	5 W
Indoor access point maximum power	0.1 W
Maximum bandwidth B^{max}	100 MHz
Center carrier frequency f_c	28 GHz
Outdoor power coefficient α_{OBS}	50
Indoor power coefficient α_{IBS}	0.02
Outdoor user position in polar coordinates	(90 m, 160^o)
Indoor user position in polar coordinates	(160 m, 160^o)
Indoor access point position in polar coordinates	(165 m, 160^o)
Inter base station distance R	300 m
Shadowing X_σ	N(0,9.6) dB
Fast fading F	X_2^2 dB
Penetration loss L_{pen}	20 dB

Using the simulation parameters given in Table I and Equation (1) we have generated the simulation results for SE as given in Figure 2. The averaged SE achieved by an outdoor user which is served by an outdoor base station is shown in Figure 2.

The SE shown in Figure 2 on low transmit power regime of BS increases rapidly achieving the value of 14 bits/s/Hz until the BS transmit power attains the value of 1.5 W. After this value the SE increases only for 1 bit/s/Hz until the BS attains the maximum transmit power of 5 W. This difference in SE occurs due to the inter cell interference which increases while the transmit power is increased. The averaged SE achieved by an indoor user which is connected to an IBS is shown in Figure 3. Comparing the simulation results shown in Figure 2, in Figure 3 one can notice that there is higher SE achieved by a user which is connected to an IBS than the user which is connected to the OBS. This stems from the fact that the IBS is isolated due to the inter cell interference. To analyze the trade-off between EE and SE, we have presented the simulation results as in the following. The simulation results which show the trade-off between EE and SE for an outdoor user are provided in Figure 4.

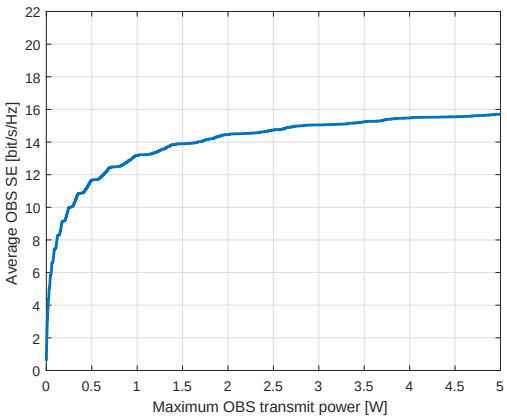

Fig. 2. Averaged SE for the outdoor user.

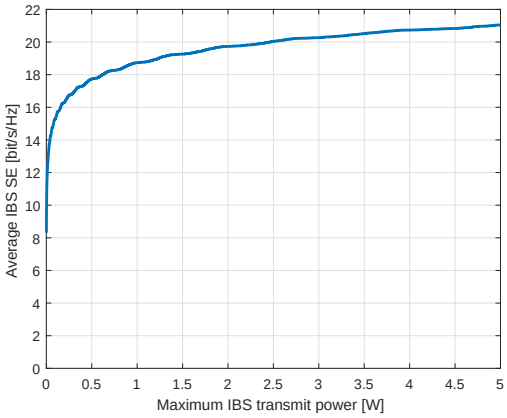

Fig. 3. Averaged SE for the indoor user.

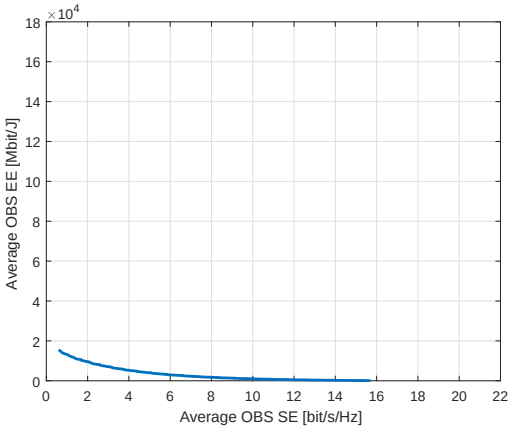

Fig. 4. Averaged trade-off between EE and SE for the outdoor user.

Analyzing the simulation results shown in Figure 4, we conclude that increasing the EE results in decreasing the SE and vice versa. Similarly, in Figure 5, we have shown the simulation results for the trade-off between EE and SE for a user served by an IBS.

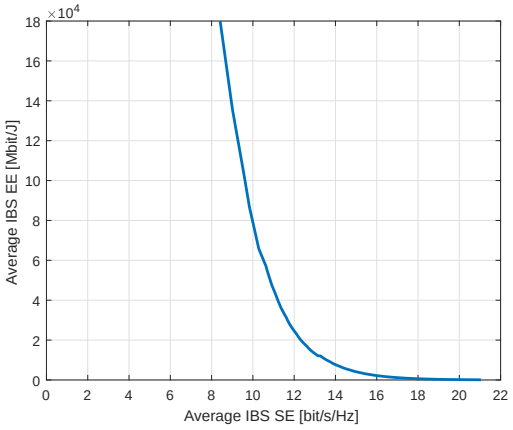

Fig. 5. Averaged trade-off between EE and SE for the indoor user.

The simulation results shown in Figure 5, indicate that same perception for the trade-off between EE and SE as for the outdoor user. Comparing the simulation results shown in Figure 4 for the outdoor user with the simulation results shown in Figure 5 for the outdoor user, we conclude that higher EE is achieved when the user is connected to the IBS than the user connected to the OBS. The comparison of SE achieved by the indoor user compared with the SE achieved by the outdoor user is shown in Figure 6.

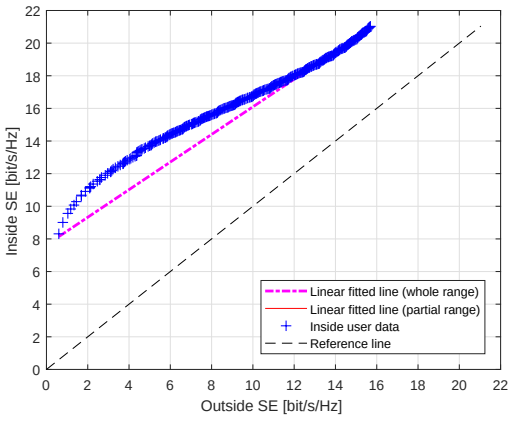

Fig. 6. indoor SE versus outdoor SE.

We apply descriptive statistics for this analysis by using Quantile-Quantile plots (Q-Q). This analysis ensures a fair comparison between two scenarios and provides an analysis to benchmark between different conditions of the mobile users. The dashed black line shown in Figure 6 is used as reference and shows the information of data samples gathered during simulations which correspond to the outdoor user. The blue plus scatters create a consistent curve in SE analysis and correspond to the data samples gathered for the indoor user. This variation is a strong indication of significant difference between two scenarios, thus the indoor user outperforms the outdoor user. Since the curve is almost linear (parallel to the reference line), we conclude that the distributions of both scenarios derived from the proposed optimization algorithm are almost similar, and they only change in statistical mean. The statistical mean calculated as the average of SE, shows $9\,\mathrm{bits/s/Hz}$ higher SE for the indoor user. Note, the pink dashed line is the fitted line of the distribution data for the indoor user. Similarly, the comparison of EE achieved by the indoor user compared to the EE achieved by the outdoor user is shown in Figure 7 and we use again the Q-Q analysis to benchmark between two scenarios.

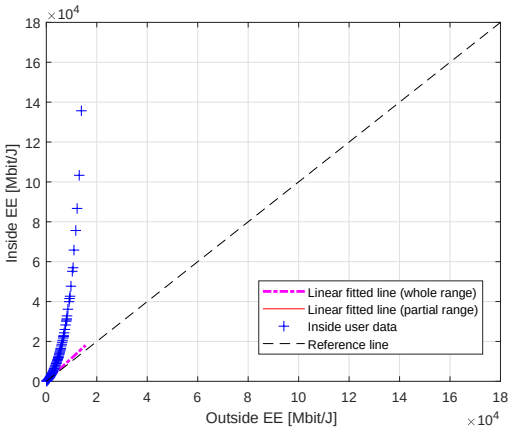

Fig. 7. indoor EE versus outdoor EE.

However, in this case we have a different situation which we pay attention. First, the distributions of data samples gathered by simulations change drastically. Second, in low regime of EE (both users), up to $7\,\mathrm{Gbit/J}$, the distributions are similar, indicating that that there is substantial difference. This difference is around $1\,\mathrm{Gbit/J}$ and indoor user outperforms the outdoor user. Third, in low regime of EE (outdoor user) up to $20\,\mathrm{Gbit/J}$, the values of indoor user are $20\,\mathrm{Gbit/J}$ higher in EE (the outliers are ignored). This big gap is created due to the very low values of SE in indoor user which correspond to high SE for outdoor user (but low EE).

V. Conclusion

In this paper we evaluated the performance of a 5G cellular network in terms of SE (Spectral Efficiency) and EE (Energy Efficiency) achieved by an indoor and outdoor user under optimal power allocation. Using the dual decomposition techniques, we derived the equation for the optimal power allocation in a water-filling like manner. We applied the water-filling like power allocation to optimally allocate the power to the users which resulted in an increase of the SE

and EE. Simulation results show higher SE and EE is achieved by the indoor user which is served by the IBS (Indoor Base Station) compared to the outdoor user which is served by the OBS (Outdoor Base Station). The indoor user outperforms in average of $9\,\mathrm{bits/s/Hz}$ the outdoor user in terms of SE. On the other hand, considering 2-user network, the EE can be as large as $20\,\mathrm{Gbit/J}$ at indoor user. Moreover, we investigated the trade-off between EE and SE by simulations. The simulation results show strong behaviour of EE and SE such that with increasing EE, the SE is decreased and vice versa.

ACKNOWLEDGMENT

The authors would like to thank Taulant Berisha from Vienna University of Technology for his fruitful comments.

REFERENCES

[1] Ericsson, "*Ericsson Mobility Report* ," Ericsson, Tech. Rep., August. 2017.

[2] U. F. R. 44, "*Mobile traffic forecasts 2010-2020 report*," UMTS Forum, Tech. Rep., Jan. 2011.

[3] Cisco, "*Cisco Visual Networking Index: Global Mobile Data Traffic Forecast Update 20162021 White Paper*," Ciso, Tech. Rep., March 28. 2017.

[4] N. Panwar, S. Sharma, and A. K. Singh, "A survey on 5g: The next generation of mobile communication," *Physical Communication*, vol. 18, pp. 64–84, 2016.

[5] J. G. Andrews, S. Buzzi, W. Choi, S. V. Hanly, A. Lozano, A. C. K. Soong, and J. C. Zhang, "*What Will 5G Be?*" *IEEE Journal on Selected Areas in Communications*, vol. 32, no. 6, pp. 1065–1082, Jun. 2014.

[6] Y. Chen, S. Zhang, S. Xu, and G. Y. Li, "Fundamental trade-offs on green wireless networks," *IEEE Communications Magazine*, vol. 49, no. 6, 2011.

[7] C. Xiong, G. Y. Li, S. Zhang, Y. Chen, and S. Xu, "Energy- and spectral-efficiency tradeoff in downlink ofdma networks," *IEEE transactions on wireless communications*, vol. 10, no. 11, pp. 3874–3886, 2011.

[8] C. He, B. Sheng, P. Zhu, and X. You, "Energy efficiency and spectral efficiency tradeoff in downlink distributed antenna systems," *IEEE Wireless Communications Letters*, vol. 1, no. 3, pp. 153–156, 2012.

[9] Z. Zhou, M. Dong, K. Ota, J. Wu, and T. Sato, "Energy efficiency and spectral efficiency tradeoff in device-to-device (d2d) communications," *IEEE Wireless Communications Letters*, vol. 3, no. 5, pp. 485–488, 2014.

[10] R. Q. Hu and Y. Qian, "An energy efficient and spectrum efficient wireless heterogeneous network framework for 5g systems," *IEEE Communications Magazine*, vol. 52, no. 5, pp. 94–101, 2014.

[11] B. Maloku, B. Krasniqi, and F. Ademaj, "Optimizing the energy efficiency for future 5g networks," in *Systems, Signals and Image Processing (IWSSIP), 2016 International Conference on*. IEEE, 2016, pp. 1–5.

[12] S. Chatterjee, S. P. Maity, and T. Acharya, "Energy efficient cognitive radio system for joint spectrum sensing and data transmission," *IEEE Journal on Emerging and Selected Topics in Circuits and Systems*, vol. 4, no. 3, pp. 292–300, Sept 2014.

[13] M. Dai, H. Y. Kwan, and C. W. Sung, "Linear network coding strategies for the multiple access relay channel with packet erasures," *IEEE Transactions on Wireless Communications*, vol. 12, no. 1, pp. 218–227, January 2013.

[14] M. Dai, S. Zhang, B. Chen, X. Lin, and H. Wang, "A refined convergence condition for iterative waterfilling algorithm," *IEEE Communications Letters*, vol. 18, no. 2, pp. 269–272, February 2014.

[15] C. Luo, G. Min, F. R. Yu, M. Chen, L. T. Yang, and V. C. M. Leung, "Energy-efficient distributed relay and power control in cognitive radio cooperative communications," *IEEE Journal on Selected Areas in Communications*, vol. 31, no. 11, pp. 2442–2452, November 2013.

[16] Y. Shi, L. Zhang, Z. Chen, Y. Gong, and G. Wu, "Optimal power allocation for af full-duplex relay in cognitive radio networks," in *2013 IEEE Globecom Workshops (GC Wkshps)*, Dec 2013, pp. 322–327.

[17] S. Wang, R. Ruby, V. C. Leung, and Z. Yao, "Energy-efficient power allocation for multi-user single-af-relay underlay cognitive radio networks," *Computer Networks*, vol. 103, pp. 115–128, 2016.

[18] S. Wang and H. Ji, "Distributed power allocation scheme for multi-relay shared-bandwidth (mrsb) wireless cooperative communication," *IEEE Communications Letters*, vol. 16, no. 8, pp. 1263–1265, August 2012.

[19] G. Y. Li, Z. Xu, C. Xiong, C. Yang, S. Zhang, Y. Chen, and S. Xu, "*Energy-efficient wireless communications: tutorial, survey, and open issues*," *IEEE Wireless Communications*, vol. 18, no. 6, pp. 28–35, Dec. 2011.

[20] B. Krasniqi, M. Wolkerstorfer, C. Mehlführer, and C. F. Mecklenbräuker, "Sum-rate maximization for multiple users in partial frequency reuse cellular networks," in *GLOBECOM Workshops (GC Wkshps), 2010 IEEE*. IEEE, 2010, pp. 814–818.

[21] B. Krasniqi., "*Partial Frequency Reuse for Long Term Evolution*," Ph.D. dissertation, PhD thesis, E389, Vienna University of Technology, 2011.

[22] B. Krasniqi, M. Wolkerstorfer, C. Mehlführer, and C. F. Mecklenbräuker, "Sum-rate maximization by bandwidth reallocation for two users in partial frequency reuse cellular networks," in *Signals, Systems and Computers (ASILOMAR), 2010 Conference Record of the Forty Fourth Asilomar Conference on*. IEEE, 2010, pp. 521–525.

[23] T. Berisha, P. Svoboda, S. Ojak, and C. F. Mecklenbräuker, "Cellular Network Quality Improvements for High Speed Train Passengers by on-board Amplify-and-Forward Relays," in *13th International Symposium on Wireless Communication Systems (ISWCS)*, Sept 2016, pp. 325–329.

[24] ——, "Seghyper: Segmentation- and Hypothesis based Network Performance Evaluation for High Speed Train users," in *2017 IEEE International Conference on Communications (ICC)*, May 2017, pp. 1–6.

[25] ——, "Benchmarking In-Train Coverage Measurements of Mobile Cellular users," in *VTC Fall 2017 - IEEE 86th Vehicular Technology Communications*, Sept 2017.

[26] T. Berisha, G. Artner, B. Kransiqi, B. Duriqi, M. Mucaj, S. Berisha, P. Svoboda, and C. F. Mecklenbräuker, "Measurement and Analysis of LTE Coverage for Vehicular Use Cases in Live Networks," in *IEEE APWC - APS Topical Conference on Antennas and Propagation in Wireless Communications*, Sep 2017.

[27] T. S. Rappaport., "*5G Channel Measurements and Models for Millimeter-Wave Wireless Communications*." *NYU Polytechnic School of Engineering, Brooklyn, New York, North American 5G Workshop*, November 2014.

[28] ITU-R., "*Propagation data and prediction methods for the planning of indoor radiocommunication systems and radio local area networks in the frequency range 900 MHz to 100 GHz*," ITU, Electronic Publication Geneva,, Tech. Rep., 2012.

[29] S. Boyd and L. Vandenberghe., *Convex Optimization*. Cambridge University Press, 2004.

[30] H. Turnbull, *Theory of Equations, fourth edition*. Oliver and Boyd, London, 1974.